CHINESE JOURNAL OF PHYSICS VOL. 52, NO. 1-I February 2014

Entanglement Percolation of Small-World Quantum Networks

Yuanyuan Feng, Lei Zhou, Liang Wu*, and Shiqun Zhu†

School of Physical Science and Technology,
Soochow University, Suzhou, Jiangsu 215006, China
(Received May 23, 2013; Revised June 29, 2013)

The effects of small-world network topology on entanglement percolation are investigated. From both classical and quantum entanglement percolation, it is found that the reduction in the percolation threshold is strongly related to the decrease of the average distance. The percolation threshold and average distance follow a power law functional relation. Moreover, a phase transition occurs from a slow reduction in the sparse-connection regime to a rapid reduction in the dense-connection regime. These findings may be helpful for a better understanding the long-distance entanglement preparation in future small-world quantum networks.

DOI: 10.6122/CJP.52.90 PACS numbers: 03.67.Bg, 64.60.ah

I. INTRODUCTION

Recently, much attention has been paid to quantum networks due to their various applications, from quantum cryptography and quantum teleportation to distributed quantum computing [1, 2]. The basic ingredient is the so-called no-cloning theorem, namely it is impossible to crack the quantum cryptography without being detected [3]. To realize these applications one of the important problems is to establish distributed entanglements between distant nodes [4].

In recent years several schemes of long-distance distributed quantum entanglement have been proposed [5]. They may require some additional quantum devices. These devices take roles like the repeaters and memories in classical communication systems [6–10]. By these means the problem of the exponential decay of entanglement with distance can be solved. Much effort has been devoted to improving the quality of these devices [11, 12].

Meanwhile some methods of preventing the rapid decay of long-distance entanglement were proposed [4] by utilizing local operations and classical communication (LOCC) [3]. Partially entangled states [12] can be converted into a maximally entangled state (singlet for short) with a so-called "singlet conversion probability" (SCP) [5, 13–15]. When SCP exceeds a threshold, a giant connected component (GCC) spanning a large fraction of a network may emerge [13]. The problem of long-distance entanglement establishment on quantum networks can be mapped into a phase transition problem in classical statistical physics. This is called the classical entanglement percolation (CEP) protocol. The threshold value strongly depends on the structural topologies of the substrate of the quantum networks. It

* Corresponding author, Electronic address: liangwu@suda.edu.cn
† Corresponding author, Electronic address: szhu@suda.edu.cn

is interesting to note that some local well-designed quantum operations can both reduce the threshold values and increase the size of the GCC [11, 13]. The latter is called the quantum entanglement percolation (QEP) protocol.

It is very plausible that a future quantum network may have a complex topology [16–18] resembling that of existing classical real communication networks, because they are very likely to be used in the quantum regime [19–22]. Small-world is one of the most important features extensively studied in classical real networks [23, 24]. However, the effects of this important topological feature on quantum networks are not well known.

In this paper, the effects of the small-world topological feature on both classical and quantum entanglement percolation are investigated. In Section II, the entanglement establishment in a small-world network is presented. The classical and quantum entanglement percolation is introduced. In Section III, the equilibrium statistical ensembles of Watts-Strogatz (WS) small-world networks [25] are analyzed using numerical methods when the average distances, the degree, and the rewired links number are varied. The size of the giant connected component and the singlet conversion probability are investigated. A discussion concludes the paper.

II. ENTANGLEMENT IN SMALL-WORLD QUANTUM NETWORK

A typical quantum network is composed of N nodes (sites) and E edges (quantum channels) connecting them. Each node is a "quantum repeater" [3, 8, 10] having several qubits. Two nodes are pairwise connected by sharing a pure but partially entangled state, $|\psi\rangle^{\otimes 2}$, $|\psi\rangle = \sqrt{\lambda_0}|00\rangle + \sqrt{\lambda_1}|11\rangle$ being a two-qubit state with Schmidt coefficients $\sqrt{\lambda_0} \geq \sqrt{\lambda_1} \geq 0$ [4, 5, 14].

The Schmidt coefficient λ_1 determines the probability $\varphi_{ij} = \min(1, 2\lambda_1)$ [3] that the maximum entanglement can be established between two nodes i and j. This probability is often called the singlet conversion probability (SCP) [14]. Multiple entanglement may be presented between a pair of nodes with more than one qubit-pair. For example, if the number of qubit-pairs are 2 between the nodes i and j, the SCP is $\varphi = \min(1, 4\lambda_1 - 2\lambda_1^2)$, with the Schmidt coefficients λ_0, $\sqrt{\lambda_0\lambda_1}$, $\sqrt{\lambda_0\lambda_1}$, λ_1 [5].

The quantum entanglement establishment in a quantum network system can be mapped into a percolation problem in classical statistical physics [19, 23–26]. Two seemingly separate types of graphs, statistical graphs and entanglement graphs, become related, using the following methods which can be applied almost directly to the quantum entanglement established in a quantum network system.If any randomly chosen pairs of nodes are in the GCC in an entanglement graph, a sequence of successive LOCC operations on the paths between these two nodes can always successfully lead to a maximum entanglement between them [19]. Therefore, entanglement establishment in a wide range of networks can be realized if a spanning subset over a major fraction of nodes emerges. This protocol for long-distance entanglement establishment on quantum networks is often called classical entanglement percolation (CEP) [5, 14]. For the limiting case of $\varphi = 0$, nodes are bare without any links in the graph representation, entanglement establishment is impossible

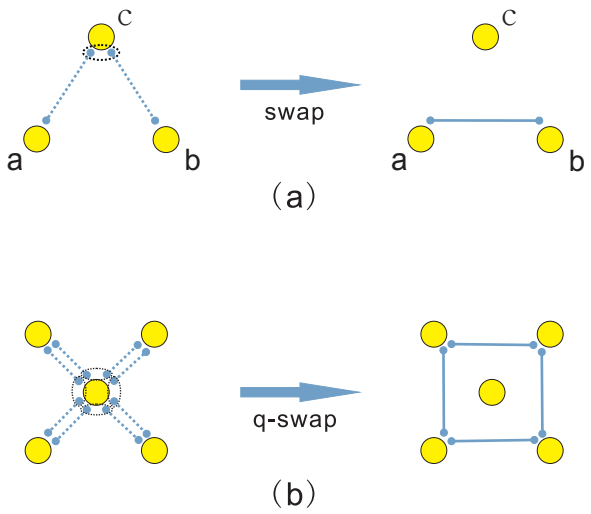

FIG. 1: (a) Schematic representation of the entanglement swapping operation. The central node c shares state $|\psi\rangle$ with nodes a and b initially. After a Bell state measurement is performed on c, node c becomes disentangled from a and b, in return an entangled state between a and b of the same averaged SCP is established. (b) Schematic representation of a "4-swap" operation as an example of a "q-swap" operation. An initial star structure with 4 branches is converted into a rectangular structure by the operation.

by any protocol. As φ is increased, several small connected components of nodes emerge one by one. They emerge with each other as φ is increased further. Eventually, when a threshold is exceeded, $\varphi \geq \varphi_c$, a critical phenomenon takes place and a giant connected component spanning most of the network emerges [13]. If all the initial partially entangled states can be successfully converted into singlets, i.e., $\varphi = 1$, the GCC is exactly the whole network. The relative size of the GCC, denoted by $S = \frac{N_{GCC}}{N}$, is also $S = 1$ in the limiting case. Here N is the total nodes number and N_{GCC} is the number of nodes in the GCC. However, such a limiting case in general cannot be reached in practice, since any environmental disturbances and quantum noises can induce decoherence effects. A thermal energy of small amount by virtue of the environmental assistance may break down the carefully prepared entanglements thoroughly [8, 11, 12].

The establishment of quantum communications over long distance can be achieved by a simple entanglement swapping procedure. The "SWAP" operations and a quantum Internet [20, 21, 27] are schematically shown in Fig. 1(a). A central node c shares state $|\psi\rangle$ with nodes a and b. After node c performs a Bell state measurement, c becomes disentangled from both a and b, while in return a and b are entangled with the same averaged SCP as $|\psi\rangle$ [5, 13].

In addition, some deliberately designed local quantum operations are performed to change the network structural topology, so that the threshold value φ_c can be reduced and the size of the GCC can be raised. Thus, entanglement swapping operations of "q-swap" are performed between a q-degree node and its neighbors. Such a "q-swap" is schematically

shown in Fig. 1(b). It can change an initial q-star structure to a q-cycle. Such "q-swap" operations are performed deliberately ahead of the percolation process. The network structures are changed due to these operations, and consequently entanglement percolation properties can be improved. This type of percolation protocol is often referred to as quantum entanglement percolation (QEP) [13, 19]. That is, the only difference of QEP from CEP is that the additional "q-swaps" are introduced in QEP.

Both CEP and QEP can be applied to a classical equilibrium statistical ensemble of small-world network models. Networks of different strengths of both small-world and clustering features can be generated as follows [25, 28, 29]: Firstly, N nodes are organized in a ring. Each node in this ring is connected to the K nearest neighbors on the left hand side, and K nearest neighbors on the right. Therefore the total number of links is $E = NK$ and the mean degree (the average number of links one node has) is $\langle k \rangle = 2K$. Secondly, each link is rewired randomly with a probability P. Neither repeat nor self linkages are allowed. The rewired links are often called shortcuts, since these rewired links can dramatically decrease the average distance L.

The local clustering coefficient c_i is often used to measure how often the neighbors of node i are also connected with each other with $c_i = \frac{2e_i}{k_i(k_i-1)}$, where k_i is the number of the links attached to node i and e_i is the number of edges between the nearest neighbors of node i. The mean value over all nodes is often referred to as the clustering coefficient C with $C = \langle c_i \rangle = \frac{1}{N}\sum_{i\in N} c_i$ [30].

The average distance L is scaled as $L \sim (1/P)\ln(NP)$ [26] and the average clustering is $C(P) = \frac{3(K-2)}{4(K-1)}(1-P)^3$ [31]. Here, the effects of small-world on entanglement percolation are investigated.

III. CLASSICAL AND QUANTUM ENTANGLEMENT PERCOLATION

III-1. Simulation Procedures

The procedure for numerical simulations of CEP is as follows. Nodes are pairwise connected by sharing pure but partially entangled states. To simulate the entanglement percolation process, every entangled state is converted into a singlet with a singlet conversion probability ϕ. After that, one has to look for all the connected components in the network. A connected component is a subgraph where any two nodes are connected by at least one path and to which no more nodes can be added without losing this property [13]. Note that many small components may coexist when the probability ϕ is at a low value. So a typical giant connected component having a size of the same order with the whole network is present only when ϕ is sufficiently large. Here the largest connected component is found out and is considered as the candidate giant connected component. Its relative size S can be depicted as a function of ϕ.

Compared with CEP, the only difference in the numerical simulation procedure for QEP is that a deliberately designed transformations by quantum preprocessing "q-swaps" operations are carried out ahead of the percolation process. In a "q-swaps" operation,

swapping transformations are performed successively between a central target node of degree q and its neighbors, thus changing an initial "q-star" to a "q-cycle". The node where one starts applying the q-swap operation is randomly chosen and the network is traversed.

The newborn edges after a "q-swaps" operation are not in a state $|\psi\rangle$ and cannot be reused. "q-swaps" operations therefore cannot be repeated at the neighboring nodes of the target nodes [5, 13]. For this reason, not all nodes of degree q are suitable targets of "q-swaps" [22]. Here the "q-swaps" are done by traversing the networks with a breadth-first search [13, 22]. That is, start applying "q-swaps" at a randomly chosen node if the node degree is one of the target degrees. Explore all the neighboring nodes at distance 1, 2,..., until all the nodes have been visited. To make clear the possible advantage of QEP over CEP, here the "$2, 3, ..., k_{max}$-swaps" are performed. The exact number of "q-swaps" operations depends on the details of the network, and consequently the different realizations of small-world network generation. It turns out that 400 ± 8 "q-swaps" operations are made for the small-world networks of $N = 4000$ in our simulations. In addition, the number of "q-swaps" operations is also close to this value if "$2, 3, ..., \langle k \rangle$-swaps" operations are made. This may be due to the saturation effect arising when traversing the networks [13, 22]. All the results below are averaged over 50 different network realizations.

III-2. Effects of CEP and QEP

The effects of classical and quantum entanglement percolation on WS small-world networks can be evaluated by the size S of GCC, the average distance L, and the clustering coefficient C when the singlet conversion probability φ and the relative shortcut number P are varied.

In Fig. 2, the size S of GCC as a function of the singlet conversion probability φ is plotted for CEP (dotted lines) and QEP (solid lines), respectively, when the relative shortcut number P (P also denotes the rewiring probability) is varied. There is a continuous transition when φ exceeds the threshold value, no matter what set of parameters is chosen. In numerical calculations throughout this paper, the threshold φ_c is defined as the value of φ such that $S = \frac{1}{e}$. In the insets it is seen that the threshold value is strongly related to how many shortcuts P there are in the network and what protocol is applied. It is seen that the threshold φ_c of QEP is smaller than that of CEP when P increases. The reduction is not very large, e.g., the relative decrease of the threshold φ_c is as small as 3.8% for $P = 0.5$. However, such a decrease is sometimes still nontrivial, especially in the situation where the amount of initial entanglement is so small that other methods become nearly impossible to realize long-distance entanglement establishment, while the entanglement percolation protocols of both CEP and QEP still work by virtue of complex network structures [13, 22].

The dependence of the threshold value φ_c (i.e., the critical point of percolation), the average distance L, and the clustering coefficient C on the relative shortcut number P is plotted in Fig. 3 for CEP and QEP, respectively. The value of φ_c is plotted in Fig. 3(a) as a function of P. From Fig. 3(a), it is clear that φ_c decreases monotonically with P, and the curve of QEP is always lower than that of CEP. That is, more shortcuts in networks can result in an improvement of entanglement percolation, and it can reduce the critical value

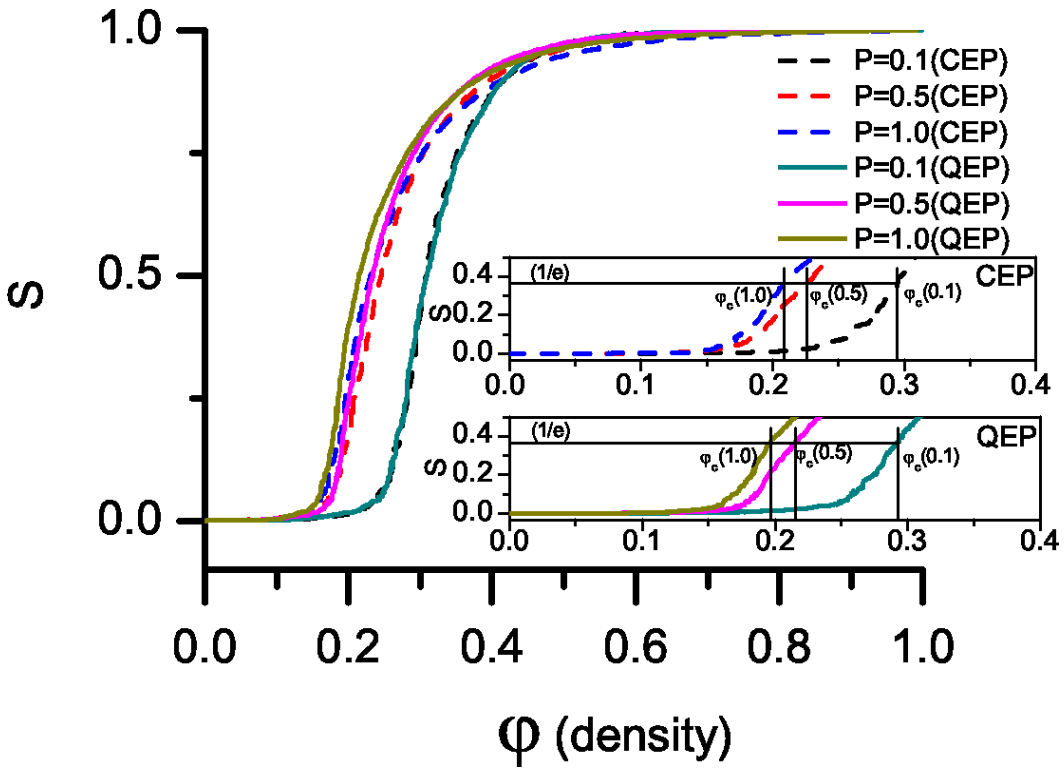

FIG. 2: (Color online) The size S of GCC is plotted as a function of the singlet conversion probability φ for CEP and QEP on WS small-world network models when the relative shortcut number P is varied. The inset enlarges the parameter region of φ around the phase transition threshold φ_c. A greater reduction of φ_c by QEP relative to that of CEP can be achieved when P is larger. The parameters are $N = 4000$, $K = 3$, $\langle k \rangle = 6$, and $E = 12000$.

for percolation from 0.294 in the limiting case of regular networks without any shortcuts to 0.210 (for CEP) and 0.200 (for QEP) in another limiting case of random networks with $P = 1$. Moreover, the reduction in φ_c is quite rapid, especially in the parameter region from $P = 0$ to $P = 0.2$. This indicates that even only a very small number of shortcuts can change the entanglement percolation properties greatly. We mention that C actually depends on the explicit realization of a rewiring process. We repeated our calculations by using different realizations, however similar results were obtained. This similarity may be due to the independence of the statistical properties of L and C on the different realizations of rewiring.

The enhancement of percolation of QEP over CEP is not obvious when P is relatively small. Therefore, additional quantum operations cannot reduce φ_c on networks of regular structures, or at least close to regular structures. Clear reduction can only be achieved when there are more than 50% of the links that are shortcuts. It is seen that the improvement of QEP over CEP is quite small, with $\frac{\phi_c(QEP)-\phi_c(CEP)}{\phi_c(CEP)} = 0.4\%$ for $P = 0.1$. This changing rate is raised to 3.8% for $P = 0.5$ and is increased further to as much as 7.4% for $P =$

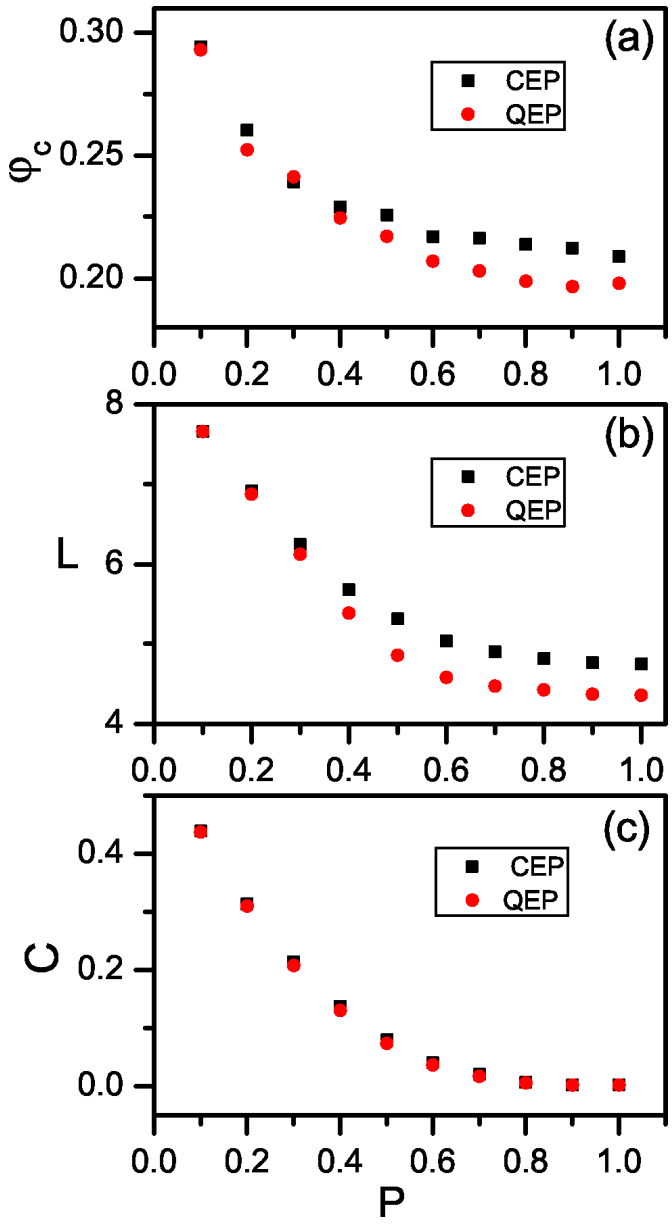

FIG. 3: (Color online) The percolation threshold φ_c, the average distance L, and the clustering coefficient C are plotted as a function of the relative shortcut number P. (a) The threshold value of φ_c is plotted as a function of P. The obvious reduction of φ_c can be seen only when the quantum entanglement of the long-distance shortcut P is more than 50%. (b) The average distance L is plotted as a function of P. The smaller average distance in QEP than CEP may account for the smaller threshold value of φ_c. (c) The clustering coefficient C is plotted as a function of P. There is almost no difference in the clustering coefficient C. The parameters are $N = 4000$ and $K = 3$.

0.9. Random rewiring can reduce and help "SWAP" operations to further reduce φ_c. In this sense network topological complexity is one of the main factors accounting for the improvement of entanglement percolation. Such amounts of reduction in ϕ_c are not large, however, they are still nontrivial in the long-distance entanglement establishment.

The average distance L is plotted as a function of P in Fig. 3(b). Similar to Fig. 3(a), L decreases monotonically as P increases. The curve of QEP is lower than that of CEP. That is, the average distance L is reduced further after quantum q-swap operations are performed. This indicates that the network structure becomes more compact.

The clustering coefficient C is plotted as a function of P in Fig. 3(c). Though the value of C decrease as P increases, there is almost no difference between QEP and CEP. This shows that the entanglement percolation cannot be affected by the clustering effects of small-world networks.

From the expressions of the average distance $L \sim (1/P)\ln(NP)$ [26] and the average clustering $C(P) = \frac{3(K-2)}{4(K-1)}(1-P)^3$ [31], it is clear that both L and C are decreased with P as shown in Fig. 3(b) and (c). A typical small-world network has both a small average distance and high clustering coefficient simultaneously. The network model used here has these two properties when the value of P is intermediate. The small-world property has been observed in most complex physical, biological, and social networks [30]. This property is shown to have great effects on the dynamical behavior, such as spreading processes [32] and synchronization phenomenon [33] taking place on the networked system.

The advantage of QEP over CEP is related to the decreasing network average distance, as shown in Fig. 3. We mention that the employment of quantum swap operations in QEP is not the only way to make a network more compact. The average distance L can be decreased even more directly by either increasing the number of nodes N or by decreasing the number of links E. The percolation property ϕ_c can be affected by changing both E and N. The percolation critical value φ_c is plotted as a function of the average distance L in Fig. 4 for different numbers of nodes and links.

Four networks of different sizes N are presented. When K is increased, both φ_c and L are decreased. As K is increased from $K = 3$ up to $K = 11$, networks become smaller. The power law functional relation of $\varphi_c \sim L^{\gamma}$ is clearly shown, no matter what the sizes of networks are [23–26]. There are two distinct parameter regions of K. In Region I of $K < 5$, the networks are sparse. The value of φ_c decreases slowly with L and $\gamma \approx 0.1$. There is a phase transition of φ_c. That is, when K is as large as or more than $K = 6$, the connection density φ_c drops rapidly with $\gamma \approx 2.0$. Such phase transitions taking place at about $K = 5$ is an intrinsic property and is independent of the network size N.

IV. CONCLUSIONS

The small-world effects of network structural topologies on entanglement percolation are investigated. The small-world effects which will most probably be observed in future quantum networks can greatly reduce the threshold value for the giant connected compo-

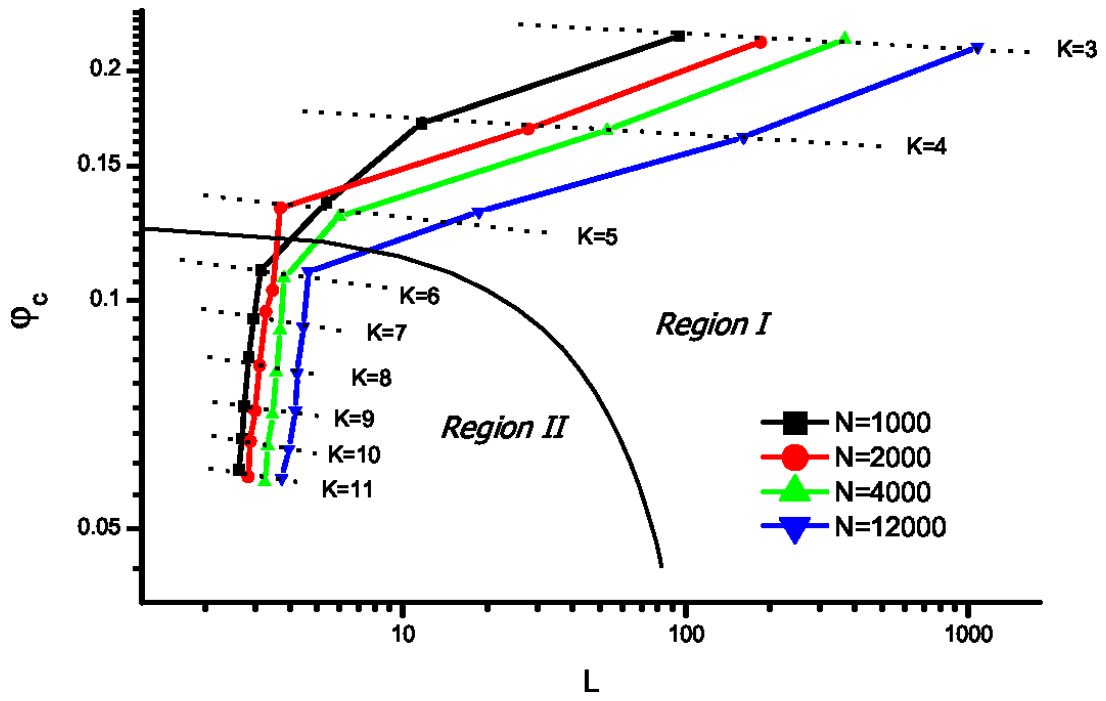

FIG. 4: The threshold value of φ_c is plotted as a function of the average distance L for varied K and different sizes N of networks. Two distinct parameter regions are clearly shown. The relative shortcut number is $P = 0.5$.

nent to emerge. Moreover, a power law scaling gives the functional relation between the threshold value and the average distance [23, 24]. The corresponding exponent having two distinct values, characterizing a phase transition phenomenon taking place from the sparse-connection regime to the dense-connection regime. It seems that such a phase transition is an intrinsic feature for small-world networks. Both its occurrence and the critical point in terms of mean degree are irrespective of the network size. These findings may be useful for a better understanding of the long-distance entanglement preparation in the context of small-world quantum networks.

Acknowledgements

The financial supports from the National Natural Science Foundation of China (Grant No. 11074184, 11204197, 11105095, 11205111), the Natural Science Foundation of Higher Education Institutions of Jiangsu Province (Grant No. 11KJB140008), and the Priority Academic Program Development of Jiangsu Higher Education Institutions (PAPD) are gratefully acknowledged.

References

[1] L.-M. Duan, M. D. Lukin, J. I. Cirac, and P. Zoller, Nature **414**, 413 (2001). doi: 10.1038/35106500

[2] H. J. Kimble, Nature **453**, 1023 (2008). doi: 10.1038/nature07127

[3] G. Vidal, Phys. Rev. Lett. **83**, 1046 (1999). doi: 10.1103/PhysRevLett.83.1046

[4] S. Perseguers, D. Cavalcanti, G. J. Lapeyre, Jr., M. Lewenstein, and A. Acín, Phys. Rev. A **81**, 032327 (2010). doi: 10.1103/PhysRevA.81.032327

[5] G. J. Lapeyre, Jr., J. Wehr, and M. Lewenstein, Phys. Rev. A **79**, 042324 (2009). doi: 10.1103/PhysRevA.79.042324

[6] L. Hartmann, B. Kraus, H.-J. Briegel, and W. Dür, Phys. Rev. A **75**, 032310 (2007). doi: 10.1103/PhysRevA.75.032310

[7] L. Jiang *et al.*, Phys. Rev. A **79**, 032325 (2009). doi: 10.1103/PhysRevA.79.032325

[8] H.-J. Briegel, W. Dür, J. I. Cirac, and P. Zoller Phys. Rev. Lett. **81**, 5932 (1998). doi: 10.1103/PhysRevLett.81.5932

[9] W. Dür, H.-J. Briegel, J. I. Cirac, and P. Zoller, Phys. Rev. A **59**, 1 (1999).

[10] N. Gisin and R. Thew, Nature Photonics **1**, 165 (2007). doi: 10.1038/nphoton.2007.22

[11] S. D. Barrett and T. M. Stace, Phys. Rev. Lett. **105**, 200502 (2010). doi: 10.1103/PhysRevLett.105.200502

[12] J. Modławska and A. Grudka, Phys. Rev. Lett. **100**, 110503 (2008).

[13] M. Cuquet and J. Calsamiglia, Phys. Rev. Lett. **103**, 240503 (2009). doi: 10.1103/PhysRevLett.103.240503

[14] S. Perseguers, J. I. Cirac, A. Acín, M. Lewenstein, and J. Wehr, Phys. Rev. A **77**, 022308 (2008). doi: 10.1103/PhysRevA.77.022308

[15] S. Perseguers *et al.*, Phys. Rev. A **78**, 062324 (2008). doi: 10.1103/PhysRevA.78.062324

[16] D. Alderson, J. C. Doyle, L. Li, and W. Willinger, Internet Mathematics **2**, 4 (2005).

[17] J. C. Doyle *et al.*, Proc. Natl. Acad. Sci. USA, **102**, 14497–14502 (2005). doi: 10.1073/pnas.0501426102

[18] P. Mahadevan, D. Krioukov, K. Fall, and A. Vahdat, Proceedings of the 2006 conference on Applications, technologies, architectures, and protocols for computer communications, September 11–15, 2006, Pisa, Italy.

[19] S. Broadfoot, U. Dorner, and D. Jaksch, Phys. Rev. A **82**, 042326 (2010). doi: 10.1103/PhysRevA.82.042326

[20] S. Broadfoot, U. Dorner, and D. Jaksch, EuroPhys. Lett. **88**, 50002 (2009). doi: 10.1209/0295-5075/88/50002

[21] S. Broadfoot, U. Dorner, and D. Jaksch, Phys. Rev. A **81**, 042316 (2010). doi: 10.1103/PhysRevA.81.042316

[22] M. Cuquet and J. Calsamiglia, Phys. Rev. A **83**, 032319 (2011). doi: 10.1103/PhysRevA.83.032319

[23] C. Moore and M. E. J. Newman, Phys. Rev. E **61**, 5678 (2000). doi: 10.1103/PhysRevE.61.5678

[24] C. Moore and M. E. J. Newman, Phys. Rev. E **62**, 7059 (2000). doi: 10.1103/PhysRevE.62.7059

[25] D. J. Watts and S. H. Strogatz, Nature **393**, 440 (1998). doi: 10.1038/30918

[26] M. E. J. Newman and D. J. Watts, Phys. Lett. A **263**, 341 (1999). doi: 10.1016/S0375-9601(99)00757-4

[27] J. Modławska and A. Grudka, Phys. Rev. A **78**, 032321 (2008).

[28] A. C. Potter and P. A. Lee, Phys. Rev. Lett. **105**, 227003 (2010). doi: 10.1103/PhysRevLett.105.227003

[29] D. Barmpoutis and R. M. Murray, (2010), e-print arXiv:1007.4031v1 [q-bio.MN].

[30] S. Boccaletti, V. Latora, Y. Moreno, M. Chavez, and D.-U. Hwang, Phys. Rep. **424**, 175 (2006). doi: 10.1016/j.physrep.2005.10.009
[31] A. Barrat and M. Weigt, Eur. Phys. J. B **13**, 547–560 (2000). doi: 10.1007/s100510050067
[32] M. Kuperman and G. Abramson, Phys. Rev. Lett. **86**, 2909 (2001). doi: 10.1103/PhysRevLett.86.2909
[33] M. Barahona, and L. M. Pecora, Phys. Rev. Lett. **89**, 054101 (2002). doi: 10.1103/PhysRevLett.89.054101